Reply to "Comments on 'Describing the Shape of Raindrop Size Distributions Using Uncorrelated Raindrop Mass Spectrum Parameters'"

CHRISTOPHER R. WILLIAMS,[a,b] V. N. BRINGI,[c] LAWRENCE D. CAREY,[d] V. CHANDRASEKAR,[c] PATRICK N. GATLIN,[e] ZIAD S. HADDAD,[f] ROBERT MENEGHINI,[g] S. JOSEPH MUNCHAK,[h] STEPHEN W. NESBITT,[i] WALTER A. PETERSEN,[j] SIMONE TANELLI,[f] ALI TOKAY,[k] ANNA WILSON,[l] AND DAVID B. WOLFF[j]

[a] *Cooperative Institute for Research in Environmental Sciences, University of Colorado Boulder, Boulder, Colorado*
[b] *NOAA/ESRL Physical Sciences Division, Boulder, Colorado*
[c] *Colorado State University, Fort Collins, Colorado*
[d] *University of Alabama in Huntsville, Huntsville, Alabama*
[e] *NASA Marshall Space Flight Center, Huntsville, Alabama*
[f] *Jet Propulsion Laboratory, California Institute of Technology, Pasadena, California*
[g] *NASA Goddard Space Flight Center, Greenbelt, Maryland*
[h] *University of Maryland, College Park, College Park, Maryland*
[i] *University of Illinois at Urbana–Champaign, Urbana, Illinois*
[j] *NASA Goddard Space Flight Center Wallops Flight Facility, Wallops Island, Virginia*
[k] *University of Maryland, Baltimore County, Greenbelt, Maryland*
[l] *Duke University, Durham, North Carolina*

(Manuscript received 20 February 2015, in final form 9 July 2015)

We thank Professor G. Zhang for reading our article and taking the time to submit a formal comment to the *Journal of Applied Meteorology and Climatology* (Zhang 2015). After seeing how this comment misinterprets the analysis presented in Williams et al. (2014), it is our pleasure to have an opportunity to clarify our work so that the community can appreciate the differences between Professor Zhang's work using two-parameter constrained-gamma (C-G) raindrop size distribution (DSD) models and our work using three-parameter unconstrained DSD models.

1. Introductory comments

First and foremost, a C-G distribution model, or a μ–Λ relationship, as introduced in Zhang et al. (2001, 2003) and improved in Cao et al. (2008), describes curves that pass through clusters of points. Each curve is a "best fit" curve that minimizes a mathematical constraint, represents a family of gamma DSDs, passes through the cluster of points, and is presented—in Zhang et al. (2001, 2003) and Cao et al. (2008)—without error bars or uncertainties. On the one hand, if these papers had included error bars along with their best-fit curves, then Williams et al. (2014) may not have been written or may not have passed the peer-review process. On the other hand, since these papers assumed that DSDs are described with gamma distributions and did not provide uncertainty estimates for their best-fit curves, Williams et al. (2014) presented, first, a method to estimate best-fit curves through physically meaningful DSD quantities (e.g., σ_m and D_m) that are *not constrained* to follow gamma distributions and, second, a method to deviate away from these best-fit curves that uses the concept of joint probability distribution functions (joint PDFs).

In Williams et al. (2014), the first analysis step estimated a best-fit curve that passed through a cluster of points without assuming a functional form of the DSD. If the best-fit curve was constrained to conform to a gamma distribution and the analysis was stopped at this point, then the work of Williams et al. (2014) would

Denotes Open Access content.

Corresponding author address: Christopher R. Williams, Cooperative Institute for Research in Environmental Sciences, University of Colorado Boulder, 216 UCB, Boulder, CO 80309-0216. E-mail: christopher.williams@colorado.edu

DOI: 10.1175/JAMC-D-15-0058.1

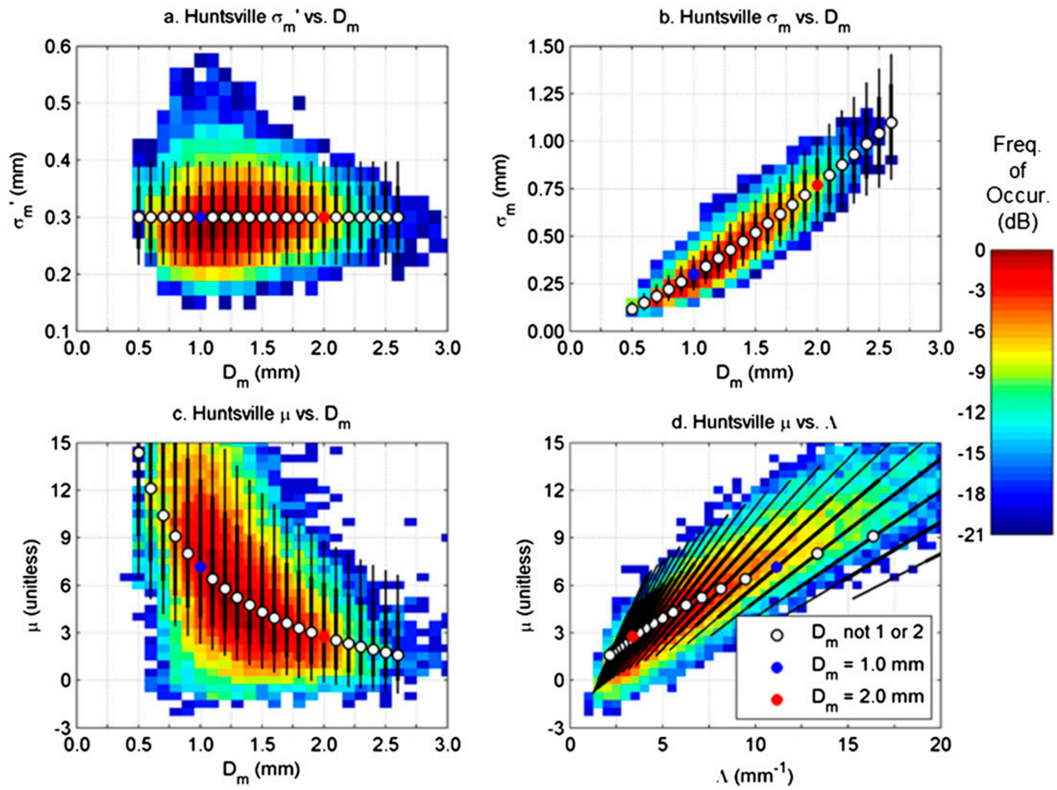

FIG. 1. Joint PDFs for narrow ranges ($\pm$0.05 mm) of mean raindrop diameter D_m shown using box-and-whisker symbols. (a) Joint PDFs of normalized mass spectrum standard deviation $\rho(\sigma'_m \mid D_m)$, (b) joint PDFs of mass spectrum standard deviation $\rho(\sigma_m \mid D_m)$, (c) joint PDFs of μ shape parameter $\rho(\mu \mid D_m)$, and (d) joint PDF of mass spectrum standard deviation $\rho(\sigma_m \mid D_m)$ mapped into the μ-vs-Λ domain. Color tiles are frequency of occurrence in logarithmic scale: the tile with the most occurrences has 0 dB, and each 50% decrease in occurrence has a 3-dB decrease on the color scale. Circles represent the mean PDF value, tips of thick lines represent $\pm$1 std dev, and tips of thin lines represent 5th and 95th percentiles.

conceptually be similar to the work presented in Zhang et al. (2001, 2003) and Cao et al. (2008) with regard to fitting a curve through a cluster of points while assuming gamma-shaped DSDs. The innovation presented in Williams et al. (2014), however, starts *after* estimating an unconstrained best-fit curve through a cluster of points by quantifying how to *deviate* from that best-fit curve by using joint PDFs.

The concept of joint PDFs is visually expressed in Fig. 1, with Figs. 1a–c containing the same information that is contained in Figs. 5c, 6a, and 6c, respectively, of Williams et al. (2014) except that the joint PDFs are shown with box-and-whisker symbols rather than free-flowing curves. The white, red, and blue dots represent discrete values of the best-fit curve passing through the cluster of points for individual values of D_m. The box-and-whisker lines represent how the data deviate away from the best-fit curve, with the thick lines representing $\pm$1 standard deviation and the thin lines representing the 5th and 95th percentiles. It is important to note that Figs. 1a and 1b show ''distribution free'' relationships that are based on observed DSD moments without assuming a functional form of the DSD shape. After it was concluded that a family of gamma distributions could represent the DSD shape [see p. 1289 in Williams et al. (2014) for more details], raw observations were mapped into the gamma parameter space of (μ, D_m) shown in Fig. 1c by using Ulbrich (1983) nontruncated gamma-distribution transformation equations. The graphics in Figs. 1a–c illustrate an important message of Williams et al. (2014)—namely, that, given a value of D_m, the dots represent the *expected value* of σ'_m, σ_m, and μ and the box-and-whisker lines represent how the data *deviate away* from the expected value.

Each joint PDF shown in Figs. 1a–c is constructed from data that are contained within a narrow range of D_m (e.g., center value $\pm$ 0.05 mm), with Fig. 1d showing the joint PDFs after a coordinate transformation into the (μ, Λ) domain is performed. To help to clarify the

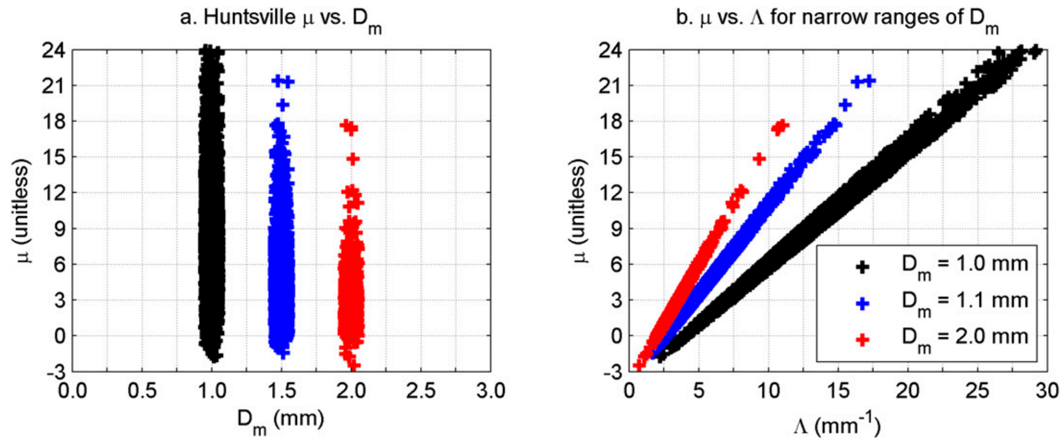

FIG. 2. Scatterplots of data for mean diameter D_m ranges centered at 1.0, 1.5, and 2.0 mm, with spread of ± 0.05 mm, (a) in the μ-vs-D_m domain and (b) in the μ-vs-Λ domain.

transformation from the (μ, D_m) domain to the (μ, Λ) domain, note that the blue and red dots have the same μ value in both Figs. 1c and 1d. In the context of "[d]escribing the shape of raindrop size distributions using uncorrelated raindrop mass spectrum parameters" [cf. title of Williams et al. (2014)], it is informative to notice that joint PDFs in Figs. 1a–c represent the spread of σ'_m, σ_m, and μ for narrow uncorrelated ranges of D_m. In contrast, joint PDFs expressed in (μ, Λ) space spread over correlated values of μ and Λ parameters. In mathematical terms and assuming nontruncated gamma distributions, this correlation is expected since the coordinate transformation is a simple relationship [Eq. (10) in Ulbrich 1983]:

$$\Lambda = (\mu + 4)/D_m, \tag{1}$$

and, because D_m is held to within a very narrow range, variations in μ manifest as variations in Λ, yielding highly correlated μ and Λ parameters.

To help to illustrate that box-and-whisker lines are derived from narrow ranges of D_m observations, Fig. 2 shows scatterplots for D_m ranges centered at 1.0, 1.5, and 2.0 mm with spread of ± 0.05 mm. Figure 2a presents the scatter in the (μ, D_m) domain, and Fig. 2b presents the scatter in the (μ, Λ) domain. The scatter in the (μ, Λ) domain is visually highly correlated and is quantified in Table 1 by listing Pearson correlation coefficients for $r(D_m, \sigma'_m)$, $r(D_m, \sigma_m)$, $r(D_m, \mu)$, and $r(\mu, \Lambda)$ using all D_m ranges containing at least 500 samples. By construction, D_m is uncorrelated with σ'_m, σ_m, and μ, with correlation-coefficient magnitudes of 0.23 or less. In contrast, μ and Λ are highly correlated, with correlation coefficients of no less than 0.996. This result indicates that when data are divided into narrow ranges of D_m the mathematical parameters of μ and Λ are highly correlated, implying that errors in one parameter will be compensated by errors in the other parameter as noted in Chandrasekar and Bringi (1987). Also, Fig. 2 highlights that DSD parameter orthogonality in one domain is not preserved after coordinate transformation into another parameter domain.

These introductory comments are summarized with three main thoughts. First, the C-G DSD model, or μ–Λ relationship (Zhang et al. 2001, 2003; Cao et al. 2008), assumes, or restricts, raindrop size distributions to be described with gamma distributions whereas σ_m–D_m relationships can be developed from raw observations without assuming a particular functional form, or shape, of the raindrop size distribution (Williams et al. 2014). Second, the work presented in Zhang et al. (2001, 2003) and Cao et al. (2008) constructs single best-fit curves that

TABLE 1. Pearson correlation coefficients estimated for narrow ranges of D_m. Columns contain the number of samples n, the D_m center value (mm) with spread of ± 0.05 mm, and correlation coefficients for $r(D_m, \sigma'_m)$, $r(D_m, \sigma_m)$, $r(D_m, \mu)$, and $r(\mu, \Lambda)$. Only intervals with over 500 samples are included in this table.

n	D_m	$r(D_m, \sigma'_m)$	$r(D_m, \sigma_m)$	$r(D_m, \mu)$	$r(\mu, \Lambda)$
795	0.70	0.01	0.22	−0.03	0.996
1340	0.80	−0.14	0.06	0.10	0.996
1904	0.90	0.02	0.23	−0.10	0.996
2455	1.00	0.05	0.23	−0.13	0.998
2694	1.10	0.03	0.20	−0.07	0.998
2576	1.20	−0.04	0.13	0.01	0.998
2332	1.30	0.02	0.17	−0.07	0.998
2088	1.40	0.05	0.20	−0.10	0.999
1822	1.50	0.00	0.16	−0.05	0.998
1587	1.60	−0.05	0.10	0.02	0.999
1204	1.70	−0.03	0.13	0.00	0.999
1039	1.80	−0.00	0.14	−0.04	0.999
787	1.90	0.01	0.14	−0.05	0.999
565	2.00	−0.02	0.11	−0.01	0.999

pass through clusters of points *without error bars or uncertainty estimates*. In contrast, Williams et al. (2014) construct a best-fit curve that passes through a cluster of points as a function of D_m and *describe how the data deviate away from that best-fit curve while keeping* D_m constant. Third, since orthogonality in one domain is not preserved after coordinate transformation, joint PDFs defined in Williams et al. (2014) within the (σ'_m, D_m), (σ_m, D_m), and (μ, D_m) domains do not translate into orthogonal joint PDFs in the (μ, Λ) domain. The rest of this reply addresses the four specific points of Zhang (2015).

2. Point 1: Similarity of μ–Λ and σ_m– D_m relationships

This particular point can be broken down into two separate concerns: 1) similarity of representing best-fit curves using μ–Λ and σ_m–D_m relationships and 2) representing deviations from best-fit curves using joint PDFs. With regard to the similarity of μ–Λ and σ_m–D_m relationships, we agree that, as long as μ–Λ and σ_m–D_m relationships represent best-fit curves passing through clusters of points and one assumes that DSD shapes are described with gamma distributions, these best-fit relationships are similar. In fact, the coordinate transformation is defined in Ulbrich (1983) for nontruncated gamma distributions. This similarity between μ–Λ and σ_m–D_m relationships *only* applies to the best-fit curves passing through a cluster of points assuming gamma-shaped DSDs and *does not* apply to deviations from those best-fit curves using joint PDFs as presented in Williams et al. (2014).

With regard to the representation of deviations from best-fit curves using joint PDFs, there is an error in the derivation leading to Eq. (5b) of Zhang (2015) that indicates a misunderstanding and misinterpretation of the joint PDFs presented in Williams et al. (2014). The derivation leading to Eq. (5a) of Zhang (2015) is correct because the variable substitutions are valid for best-fit curves, but these variable substitutions are not valid for joint PDFs that represent deviations away from the expected value *with a fixed value of* D_m. In general, the upper and lower bounds ($\sigma_m^{\text{upper\_bound}}$ and $\sigma_m^{\text{lower\_bound}}$) in Eqs. (23) and (24) of Williams et al. (2014) represent the spread of a joint PDF from the expected value in Eq. (22) ($\sigma_m^{\text{expected\_value}}$) *for fixed values of* D_m. Since the joint PDF spread is relative to the expected value using the same value of D_m, the derivation leading to Eq. (5b) of Zhang (2015) must also keep D_m constant to represent the deviation away from the best-fit curve with the same value of D_m. To be specific, for the joint PDFs presented in Williams et al. (2014), Eq. (1) of Zhang (2015) cannot be used as a general variable substitution, and the unnumbered equation before Eq. (5a) of Zhang (2015) needs to be rewritten so that μ is conditioned on D_m and is a function of both D_m and Λ:

$$\mu|_{D_m} = a^2 D_m^{2b} \Lambda^2 - 4, \tag{2}$$

where D_m is held constant for each joint PDF representing deviations away from the best-fit curve evaluated at D_m. Thus, in short, the mathematics leading to Eq. (5b) of Zhang (2015) are invalid with regard to joint PDFs presented in Williams et al. (2014) because D_m must be held constant in constructing joint PDFs.

In summary, for point 1, assuming DSD shapes are described with gamma distributions, there is similarity between μ–Λ and σ_m–D_m best-fit curves because these curves and the points they pass through can be mapped between (μ, Λ) and (σ_m, D_m) domains using coordinate transformations defined by Ulbrich (1983). In contrast, deviations away from best-fit curves defined with joint PDFs in Williams et al. (2014) do not simply map between (μ, Λ) and (σ_m, D_m) domains. Joint PDFs are defined with constant D_m values, and the coordinate transformation must maintain constant D_m values to be consistent with the work presented in Williams et al. (2014). The invalid mathematical substitution leading to Eq. (5b) of Zhang (2015) indicates a misinterpretation of how joint PDFs are transformed between domains and a misunderstanding of the way in which joint PDFs represent deviations away from the best-fit curve presented in Williams et al. (2014).

3. Point 2: Initial data QC thresholds

This particular point can also be broken down into two separate concerns: 1) quality control (QC) of disdrometer data and 2) using best-fit curves with two- or three-parameter DSD models. For disdrometer data QC, we agree that disdrometers have difficulty sampling small and large raindrops such that disdrometer datasets should retain as many valid spectra as possible. That is why Williams et al. (2014) used as little data filtering as possible before conducting any analysis, with the first QC stage verifying that spectra represented rain samples. In response to this point, reexamination of the disdrometer dataset revealed that requiring data to be in three different diameter bins is superfluous. If a spectrum had 50 raindrops, reflectivity greater than 10 dBZ, and rain rate greater than 0.1 mm h^{-1}, data were spread over three or more diameter bins.

In the peer-review process, there was concern that disdrometer small-drop truncation issues were affecting the statistics, which prompted the second and third QC stages. The ratio $X_{\max} = D_{\max}/D_m$ stems from the analysis in Ulbrich (1983) (using the ratio $D_{\max}/D_0$), which shows that, as the ratio $D_{\max}/D_0$ increases, the errors associated with using nontruncated gamma-function mathematics decrease. Figure 3b in Williams et al. (2014) illustrates that small $X_{\max} = D_{\max}/D_m$ ratio is more of an issue with spectra with small D_m and could be due to disdrometer drop truncation issues—thus, the introduction of the $X_{\max} = D_{\max}/D_m > 1.5$ threshold. The third QC stage did not remove data but calculated best-fit-curve power-law coefficients from spectra with $D_m > 1$ mm.

With regard to the second concern of using best-fit curves with two- or three-parameter DSD models, Zhang (2015) makes a compelling argument to use the sorting and averaging with two parameters (SATP) filtering method to estimate a best-fit curve passing through a cluster of points because this filter is a biased estimator that weights heavy-rain events more favorably than light-rain events. We agree that, if one uses a two-parameter DSD model, errors in the best-fit curve will propagate into the solution and the filtering process should retain the rain microphysics to match the retrieval purpose. If one is using a three-parameter DSD model as in Williams et al. (2014), however, the best-fit curve is not as critical because the best-fit curve provides an initial value and joint PDFs in Williams et al. (2014) describe a method to deviate off this best-fit curve. It is the responsibility of each team of model developers to determine how their model will deviate from the best-fit curve.

In summary, disdrometer data need to be quality controlled to ensure that they represent rain events. Within the context of two-parameter DSD models, the best-fit curve is very important because this constraint describes a two-parameter DSD shape with a single relationship. Within three-parameter unconstrained DSD models, however, the best-fit curve is not as crucial because the best-fit curve acts as an initial value from which the model can deviate as warranted by observations.

4. Point 3: Best-fit curves and deviations in probabilistic algorithms

This particular point contains two concerns: 1) whether a best-fit curve, by itself, can be used in probabilistic algorithms and 2) whether deviations from the best-fit curve can be used in probabilistic algorithms. For the first concern, we agree that a best-fit curve through a cluster of points, expressed in either the (μ, Λ) or (σ_m, D_m) domains, can be the expected value, or initial value, in probabilistic algorithms. For the second concern, we agree, within the C-G DSD framework and as discussed in the first paragraph of Zhang (2015), that probabilistic algorithms cannot deviate μ and Λ away from the constraining best-fit curve. Although we agree with this C-G constraint, we find it limiting in probabilistic algorithms that utilize observations from multiple sensors, we are concerned with statistical correlations between μ and Λ parameters as discussed in the introductory comments, and therefore in Williams et al. (2014) we provided a method to relax this constraint by using unconstrained three-parameter DSDs and joint PDFs in the (σ_m, D_m) domain in order for probabilistic algorithms to deviate away from the expected, or initial, value defined by the best-fit curve.

In summary, for point 3, we agree that μ–Λ relationships provide an expected, or initial, value for probabilistic rainfall retrieval algorithms that assume gamma-distribution DSD models. Williams et al. (2014), however, provide a method to relax that constraint within the (σ_m, D_m) domain so that probabilistic algorithms can deviate the DSD shape away from the shape defined by the best-fit curve.

5. Point 4: Typographical error in rain-rate equations

Per the suggestion of Professor Zhang, a corrigendum highlighting this typographical error was initiated in January of 2015 and was published in the April 2015 issue of the *Journal of Applied Meteorology and Climatology* (corrigendum to Williams et al. 2014).

6. Concluding remarks

Again, we thank Professor Zhang for showing interest in our work and for taking the time to formally comment on that work as presented in Williams et al. (2014). The comment has enhanced the significance of the conclusions of our original paper.

Acknowledgments. Support for this work was provided by Ramesh Kakar under the NASA Precipitation Measurement Mission and NASA Global Precipitation Mission Grants NNX13AI94G, NNX10AM54G, NNX13AF89G, NNX12AD03A, NNX10AP84G, NNX13AF86G, NNX13AJ55G, NNX13AI89G, and NNX10AH66G. A portion of this research was carried out at the Jet Propulsion Laboratory, California Institute of Technology, under a contract with the National Aeronautics and Space Administration. We also thank Editor Sandra Yuter for her suggestion to target our reply for a broad audience.

REFERENCES

Cao, Q., G. Zhang, E. Brandes, T. Schuur, A. Ryzhkov, and K. Ikeda, 2008: Analysis of video disdrometer and polarimetric radar data to characterize rain microphysics in Oklahoma. *J. Appl. Meteor. Climatol.*, **47**, 2238–2255, doi:10.1175/2008JAMC1732.1.

Chandrasekar, V., and V. N. Bringi, 1987: Simulation of radar reflectivity and surface measurements of rainfall. *J. Atmos. Oceanic Technol.*, **4**, 464–478, doi:10.1175/1520-0426(1987)004<0464:SORRAS>2.0.CO;2.

Ulbrich, C. W., 1983: Natural variations in the analytical form of the raindrop size distribution. *J. Climate Appl. Meteor.*, **22**, 1764–1775, doi:10.1175/1520-0450(1983)022<1764:NVITAF>2.0.CO;2.

Williams, R. C., and Coauthors, 2014: Describing the shape of raindrop size distributions using uncorrelated raindrop mass spectrum parameters. *J. Appl. Meteor. Climatol.*, **53**, 1282–1296, doi:10.1175/JAMC-D-13-076.1; Corrigendum, **54**, 932, doi:10.1175/JAMC-D-15-0055.1.

Zhang, G., 2015: Comments on ''Describing the shape of raindrop size distributions using uncorrelated raindrop mass spectrum parameters.'' *J. Appl. Meteor. Climatol.*, **54**, 1970–1976, doi:10.1175/JAMC-D-14-0210.1.

——, J. Vivekanandan, and E. A. Brandes, 2001: A method for estimating rain rate and drop size distribution from polarimetric radar measurements. *IEEE Trans. Geosci. Remote Sens.*, **39**, 830–841, doi:10.1109/36.917906.

——, ——, ——, R. Meneghini, and T. Kozu, 2003: The shape–slope relation in observed gamma raindrop size distributions: Statistical error or useful information? *J. Atmos. Oceanic Technol.*, **20**, 1106–1119, doi:10.1175/1520-0426(2003)020<1106:TSRIOG>2.0.CO;2.